JOURNAL OF CATALYSIS 110, 103–116 (1988)

The Simultaneous Measurement of Support, Metal, and Gas Phase Temperatures Using an *in Situ* IR Spectroscopic Technique

SANJAY SHARMA, DIRK BOECKER,[1] G. JORDAN MACLAY, AND RICHARD D. GONZALEZ[2]

Department of Chemical Engineering, University of Illinois at Chicago, Box 4348, Chicago, Illinois 60680

Received April 13, 1987

An *in situ* infrared technique has been developed and used for the simultaneous measurement of gas phase, support, and metal temperatures. This technique yields more realistic and consistent values for reaction temperatures than gas phase or mechanically attached microscopic surface thermocouples. The technique relies on monitoring the temperature-dependent vibrational frequencies of the catalyst support material during reaction. The support vibrational frequencies are calibrated with temperature. This enables one to determine the support temperature during reaction. A 1% Pt/SiO_2 catalyst using the oscillatory oxidation of CO as a reaction probe was used to understand the nature of heat transfer between the metal and the support. The results show that surface temperature oscillations are in phase with CO_2 formation. The resolution of the technique has been shown to be ±7°C, depending on the absorption frequency selected. Actual metal temperatures for a thin Pt film sample were determined by *in situ* resistivity measurements. In most cases the metal–surface temperature gradient was found to be less than the resolution of the IR technique.

INTRODUCTION

In a typical heterogeneous catalytic system a variety of temperatures can be considered. These temperatures include (1) the metal temperature, (2) the support temperature, and (3) the gas phase temperature. Because the metal temperature represents the true reaction temperature, a knowledge of its value under reaction conditions is important. Unfortunately the physical nature of the supported catalyst makes it difficult, if not impossible, to determine the metal temperature. In contrast, the gas phase and support temperatures are more readily accessible. Because large temperature gradients can exist between the metal and the gas, the use of gas phase temperatures can introduce large errors in the computation of temperature-sensitive parameters such as activation energies. The support temperature, on the other hand, may provide a better estimate of the reaction temperature. However, the possibility that large temperature gradients between the metal and the support exist has been the substance of considerable debate and the matter is far from settled.

A number of theoretical studies addressing both the nature and magnitude of the metal–support temperature gradient have been conducted in the past. Early attempts by Luss (*1*) and others (*2, 3*) at modeling the temperature profiles in metal crystallites showed that "short-term" metal–support temperature gradients could be as high as 500 to 800°C. These studies attempted to explain sintering behavior, and consequently were aimed at determining the maximum possible temperature rise within the metal crystallites. The periods of these large temperature gradients, however, are several orders of magnitude shorter than the elapsed time between successive reaction events. Therefore, these studies also concluded that the average temperature of the support was essentially equal to that of

[1] Present address: Department of Physical Chemistry, Schloßplatz 4, University of Muenster, 4400 Muenster, West Germany.

[2] To whom queries concerning this paper should be addressed.

0021-9517/88 $3.00

the metal particles. Several shortcomings of these studies were traced to the use of diffusion equations, the use of macroscopic transport coefficients, and the neglect of thermal boundary resistances at the metal–support interface (*4*). These shortcomings have raised concern regarding the conclusions reached by previous studies. More recently, Holstein and Boudart (*5*) developed a five-step mechanism to account for heat dissipation in a supported catalyst. Using realistic values for a fast exothermic reaction, a maximum value for the reduced temperature, $(T_m - T_s)/T_s$ where T_m and T_s are the metal and support temperatures respectively, is calculated to be 3×10^{-4}.

In addition to these theoretical calculations, several experimental studies aimed at measuring the metal–support temperature gradients have also been performed (*6–13*). Kember and Sheppard (*6*), using an infrared emission technique, studied the oxidation of CO over a Pd/SiO_2 catalyst. They measured what they considered to be the support temperature by placing a thermocouple in contact with the catalyst. Using this technique, a metal–support temperature gradient of 190°C was reported. However, the meaning of this temperature gradient is ambiguous because the support temperature measured by the thermocouple represents the combined effect of convective cooling by the gas flow and conductive and radiative heating by the catalyst. Because of this, the temperature measured by the thermocouple is probably somewhere in between that of the gas phase and that of the support. In a series of studies, Kaul and Wolf (*12, 13*) contacted rapid response microscopic thermocouples to the support of a Pt/SiO_2 catalyst pellet. Using a Fourier transform infrared spectrophotometer (FTIR), they were able to follow the Pt surface coverage of CO, and the rate of production of CO_2 while simultaneously measuring the catalyst support temperature. During the oscillatory oxidation of CO, pellet support temperature excursions of 150°C were observed and the temperature oscillations were correlated to the CO_2 gas phase and CO surface concentrations. They observed similar CO_2, CO phase relationships on the powdered catalyst pellet as Turner *et al.* (*14*), who had performed a similar study on Pt wires. However, due to the averaging nature of the infrared technique and due to the presence of hot spots, the results were difficult to correlate.

Clearly, the question of metal–support temperature gradients has been the subject of numerous investigations. Yet none of the studies have definitively established the nature or the magnitude of this gradient. This is mainly due to the uncertainty associated with the thermocouple derived temperatures. Techniques which incorporate physical and chemical information into the measurement of surface temperatures have a distinct advantage over mechanically attached thermocouples.

In the present study we have made use of a rapid response infrared spectroscopic technique. It has been known for some time that silicas have numerous absorption features in the mid-infrared region of the electromagnetic spectrum. Some of these features are due to strongly adsorbed species on the silica, primarily water. Others result from fundamental SiO_2 lattice vibrations and overtones (*15*). Kember and Sheppard (*16*), Kaul and Wolf (*12, 13*), and Boecker (*17*) have observed that when silica spectra recorded at various temperatures are referenced to a room temperature spectrum of the same sample, a number of temperature-dependent features are observed. These silica features were observed to increase with increasing temperature, resulting in a temperature-dependent absorption spectrum. If these absorption features are calibrated, it becomes possible to determine unknown silica temperatures by recording the spectrum of the unknown and comparing its temperature-dependent absorption band intensities to those of the calibration.

The infrared absorption technique offers a method by which Holstein and Boudart's (*5*) conclusions can be tested. As previ-

ously mentioned, Turner *et al.* (*14*) monitored Pt wire metal temperatures during the oscillatory oxidation of CO and showed that metal temperature fluctuations were directly proportional to the rate of CO_2 formation and inversely proportional to the gas phase concentration of CO downstream. By simultaneously monitoring the temperature-dependent infrared silica bands and the surface concentration of CO during the oscillatory oxidation of CO, it can be determined whether a similar relationship exists between the support temperature and the surface concentration. By observing oscillations over varying periods, conclusions regarding the nature and rate of heat transfer between the metal and the support can be made.

Because the magnitude of the metal–support temperature gradient is still unknown, a second investigation aimed at simultaneously measuring the metal and support temperatures was performed. A thin discontinuous Pt metal film was deposited onto a model catalyst surface, consisting of a thin quartz plate. The resistivity of this thin film can be calibrated as a function of temperature, much as a resistive temperature device (RTD), and used to measure *in situ* metal temperatures. Since the film is discontinuous it is also possible to record infrared spectra allowing surface species and infrared temperature-dependent carrier features to be monitored independently. By simultaneously collecting resistivity and infrared data, both the metal and the support temperatures can be determined and compared to give an idea of the magnitude of the metal–support temperature gradient.

EXPERIMENTAL

The major instrumental requirements for this study were met by Digilab FTS-40 Fourier transform spectrophotometer, a single pass flow reactor, a gas distribution system (flow system), an HP 3421A digital data acquisition system, a catalyst preparation system, a number of microcomputers for instrumental control, data storage and analysis, and a temperature programmer to control reactor gas phase temperatures. The FTIR spectrophotometer system was equipped with a narrow band, 4000 to 700-cm^{-1}, mercury–cadmium–telluride (MCT) liquid nitrogen cooled detector and a KBr beam splitter. A Motorola 68000 based microcomputer running kinetics software enable spectra to be collected as fast as 4 spectral scan/s at a resolution of 8 cm^{-1}.

In order to measure the thermocouple voltages and the thin catalyst film resistance, the HP 3421A data acquisition system equipped with a 10-channel multiplexing board and an 8-bit digital I/o board was used. This instrument was controlled by an HP 85B microcomputer. The 8-bit digital I/o board allows the system to be externally triggered by the FTIR spectrophotometer, thereby synchronizing the data collection tasks between the FTIR and the data acquisition system. An IBM-PC/AT was used to store, process, and present all of the data collected. The hardware coupled with a number of commercial and self-developed software items allow the collected data to be processed quickly.

The concentration of CO_2 in the reactor outlet could be followed using a Balzers QMG 112 quadrupole mass spectrometer or, more simply, by measuring the gas phase IR absorbance of CO_2 immediately downstream of the catalyst pellet sample.

Reactor Design

The stainless steel differential flow reactor used was similar to that published in a previous study (*16*). However, some important modifications were incorporated into the new design. It was manufactured by the Byron-Lambert Co., Franklin Park, Illinois.

The reactor is essentially a stainless steel tube capped at both ends by a CaF_2 infrared transparent flange. It has provisions for holding the catalyst pellet ring and has two ports for gas inlet and outlet. The end flanges are composed of four sections (Fig. 1). Flanges 1 and 2 allow stainless steel bel-

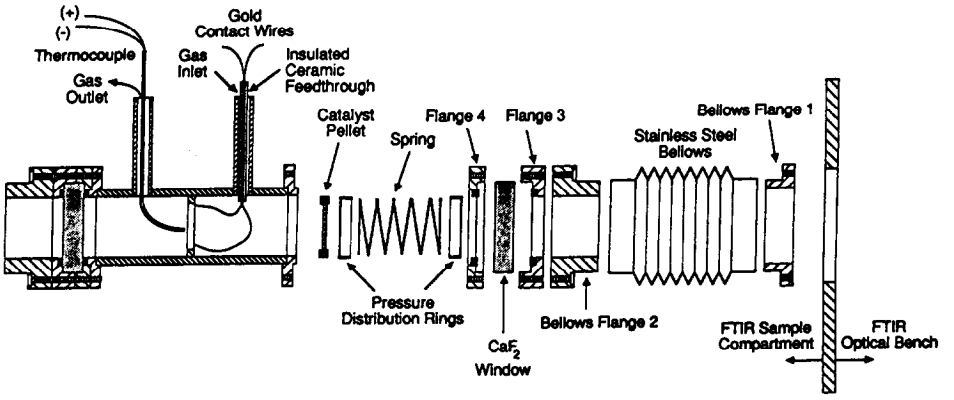

FIG. 1. *In situ* continuous flow infrared reactor.

lows to connect the FTIR optical bench to the reactor, thus isolating the CO_2 and H_2O purged environments of the FTIR from atmospheric contamination. Flanges 3 and 4 comprise the housing for a CaF_2 window which serves to seal the reactor with graphite gaskets (Grafoil, Union Carbide).

The pellet ring, when positioned in the reactor, is held in place by a fixed ring welded inside the reactor, such that the pellet is centered in the reactor, and a stainless steel compression spring held in place by the CaF_2 window flange. In order to apply even radial pressure, the spring is capped at both ends by a pressure distribution ring. In order to measure the downstream gas phase temperature a $\frac{1}{16}$-in. (1 in. = 2.54 cm) omega stainless steel-clad chromel–alumel thermocouple probe was introduced through a Swagelock fitting at the gas outlet.

Resistance measurements on the thin film catalyst samples were made by inserting two 0.005-in. gold contact wires into the reactor through two Omegatide ceramic insulated feed throughs positioned in the reactor gas inlet. Finally, the fiberglass insulated reactor could be electrically heated by 11 ft of chromel resistance wire wrapped around the reactor body. Thus, more than 1000 W of power were available for heating the reactor. Inside gas temperatures of up to 500°C with a control of ±0.5°C were obtained.

The configuration of the pellet in the reactor is such that the reactant gases are forced through the catalyst pellet, thus contacting the entire bulk of the catalyst pellet rather than just the pellet surface. In the case of the quartz-supported thin film, the sample was designed to "leak" around the edges since the quartz slide is nonporous.

Materials and Catalyst Preparation

The gases used were Linde ultrahigh purity, 99.999%. Helium, hydrogen, and oxygen were purchased from the Linox Co., Chicago, Illinois, and the 99.9% CO was supplied by Spectra Gases, Newark, New Jersey. Helium was further purified by passing it through a Supelco gas purification unit and then through an activated MnO trap. The water impurity in all gases was removed by passing them through a high surface area zeolite packed cylinder immersed in an acetone/dry ice thermal bath at −80°C.

The powdered catalyst sample was prepared by dissolving $H_2PtCl_6 \cdot 6H_2O$ (Strem Chemical) in doubly deionized water. This solution was added dropwise with continuous stirring over a 3-h period to the silica support (Cab-O-Sil, grade M-5, Cabot Corp., Boston, MA). The resultant slurry was vacuum-dried in a Rotovapor at room temperature over a 24-h period. The resulting Pt/SiO_2 catalyst had a nominal weight loading of 1% Pt. The metal dispersion as measured by the dynamic pulse method (*18*) was 30%. Sample pellets were pre-

pared by pressing 150–370 mg of the unreduced catalyst, sieved to 50–80 mesh, into a grooved stainless steel ring. The procedure was identical to that described in Ref. (*16*).

Procedure

Prior to use, the sample catalyst pellet was pretreated according to the following procedure: He was allowed to flow through the catalyst at a flow rate of 30 ml/min for 10 min in order to flush the reactor of residual gases. The temperature was then increased to 100°C at a rate of 10°C/min in flowing He. At 100°C the flow stream was switched to H_2 at the same flow rate and the temperature of the reactor was increased at a linear rate of 10°C/min to the final reduction temperature of 350°C. Following reduction in H_2 for 2 h at 350°C, the gas flowstream was switched back to He. Helium was allowed to flow through the sample at 350°C for 30 min and the catalyst was then cooled to room temperature in flowing He.

EXPERIMENTAL RESULTS

Temperature Calibration of Silica

In an infrared absorption spectrum of silica a number of features are observed (Fig. 2). Most notable of these is a large feature between 1000 and 1200 cm^{-1} resulting from the fundamental transverse and longitudinal vibrations of the SiO_2 lattice. This adsorption band in powdered silica samples is broadened due to small particle size effects and the amorphous structure of silica, to between 1500 and 900 cm^{-1} (*19*). Other absorption features resulting from fundamental lattice vibrations are located at lower frequencies, 812 and 464 cm^{-1}. However, due to the strong absorption by the CaF_2 windows below 100 cm^{-1}, these absorption frequencies are not observed. In addition to these fundamental frequencies, overtones are also present in the mid-infrared spectral region at 1625, 1860, and 2004 cm^{-1}. The remaining features in this spectrum result from absorption due to chemisorbed surface groups such as water and surface carbonates. Most notable of these is the broadband at 3744 cm^{-1} resulting from strongly adsorbed surface hydroxyl groups.

When silica spectra taken at various temperatures are referenced with a silica spectrum taken at room temperature, their temperature dependence becomes apparent. The spectral region between 1500 and 900 cm^{-1}, the overtone bands at 1625 and 1860

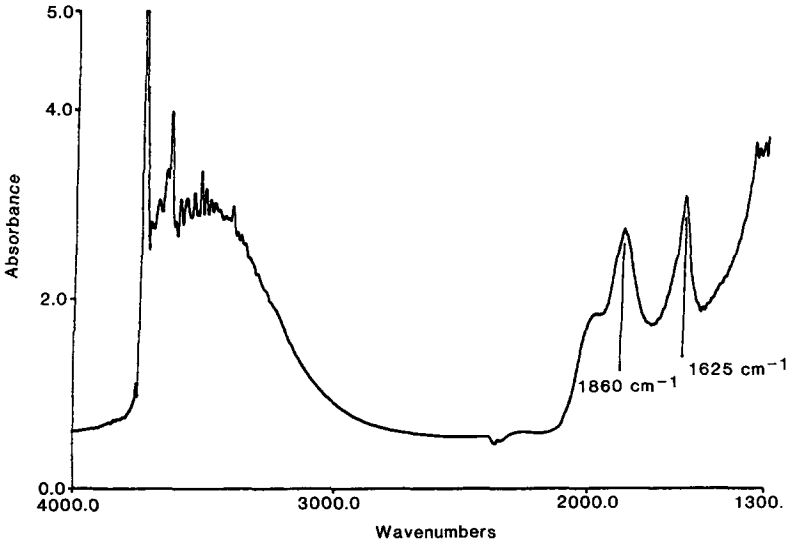

FIG. 2. Mid-infrared spectrum of powdered silica.

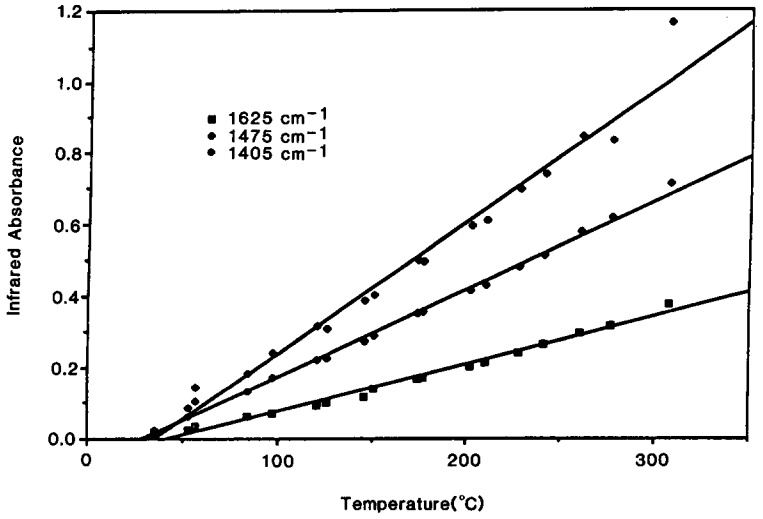

FIG. 3. Infrared calibration bands.

cm^{-1}, and also the adsorbed hydroxyl group band at 3744 cm^{-1} show a strong temperature-dependent behavior. However, the latter reflects the convoluted effects of both temperature and surface hydroxyl group concentration, which change as a result of surface dehydroxylation at elevated temperatures. Therefore the only bands which can be used for reproducible temperature calibration measurements are the ones at 1860, 1625, and 1500–1100 cm^{-1}.

If Pt/SiO_2 catalyst spectra are taken at various temperatures, the same temperature-dependent features as observed with silica result, indicating that the addition of Pt does not affect the above-mentioned infrared absorption frequencies. CO chemisorbed on Pt/SiO_2 shows two absorption bands at about 2080 and 1850 cm^{-1}. The strong high frequency band is assigned to absorption by a linear bonded CO species and the weak low frequency band is due to a bridge bonded CO species. The location of the strong band lies between 2065 and 2090 cm^{-1} depending on CO surface coverage. The weak CO band is unfortunately superimposed on the strong silica overtone. Combining all of these facts: the infrared frequencies chosen to monitor the temperature were reduced to the ones located at 1625, 1475, and 1405 cm^{-1}.

If the intensities of these frequencies are plotted as a function of temperature (Fig. 3), a thermally reversible linear relationship is obtained. Figure 3 can be considered as the sample temperature calibration and can be used to determine temperatures during subsequent reaction studies. The slope of each of these calibration curves depends on the infrared frequency selected. Different catalyst samples showed different absorbance-temperature dependencies due to changes in sample thickness. For this reason, each sample pellet was calibrated separately. However, due to the homogeneity of packing, changes in the positioning of the infrared beam within the reactor for a given catalyst pellet did not change the temperature calibration curve.

To determine the sensitivity of this infrared technique, all three infrared bands were used to measure the surface temperature under oscillatory CO-oxidation conditions. The results of this experiment for an oscillatory period of 2 min are shown in Fig. 4. Surface temperatures as measured by each of the three bands agree to within ±7°C.

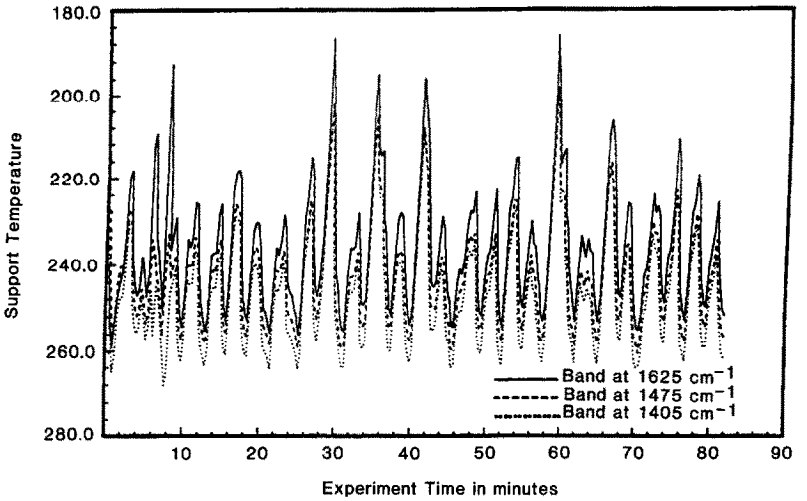

FIG. 4. Sensitivity of calculated support temperatures to selected infrared frequencies. All temperatures are in °C.

The Location of Regions Which Show CO Oxidation Instabilities

A temperature-programmed reaction study (TPR) was performed to locate the intrinsically unstable oxidation regions. These TPR experiments were carried out for five CO/O_2 ratios as follows: 2.0, 1.8, 1.4, 1.0, and 0.5. In all of the TPR experiments the total reactor gas flow rate was maintained at 100 ml/min; 50 ml/min was due to the He carrier gas flow and the remainder was due to the CO and O_2 reactant gas flows.

During a typical 2-h experimental run, 250–300 spectra were collected. Each spectrum was composed of 96 coadded scans with a final resolution of 8 cm^{-1}. The absorbance of chemisorbed CO, the support temperature used (as determined by a support temperature calibration), and the gas phase temperature for a CO/O_2 ratio of 0.5, measured downstream of the catalyst, are shown in Fig. 5. In this study the total reactor feed flow rate and the CO/O_2 ratio were held constant while the reactor gas phase temperature was increased gradually. After a gas phase temperature of 250°C was reached, the temperature programmer was switched off and the reactor was allowed to cool. The conditions under which instabilities first start to occur are apparent in Fig. 5. Other CO/O_2 ratios show similar behavior. Steady state oscillatory experiments were carried out for three CO/O_2 ratios as follows: 1.8, 1.4, and 0.5.

Oscillation Results

For a CO/O_2 ratio of 0.5, spectral data for four steady-state gas phase temperatures were collected. Each spectrum collected over a 30-min period consisted of 32 coadded interferogram scans. The resulting single-beam spectra were referenced to a room temperature spectrum of the freshly reduced catalyst pellet taken prior to the experimental run. From the four gas phase temperature runs, only the 98°C run showed detectable levels of surface CO. The steady-state oscillations in surface CO coverage and support temperature for this run are shown in Fig. 6. The rate of CO_2 formation was observed to be in phase with the surface temperature. For a CO/O_2 ratio of 1.4, the average CO surface coverage was high enough to be followed spectroscopically. Figure 7 shows the effect of gas phase temperature on the periods and amplitudes of the surface CO and support tem-

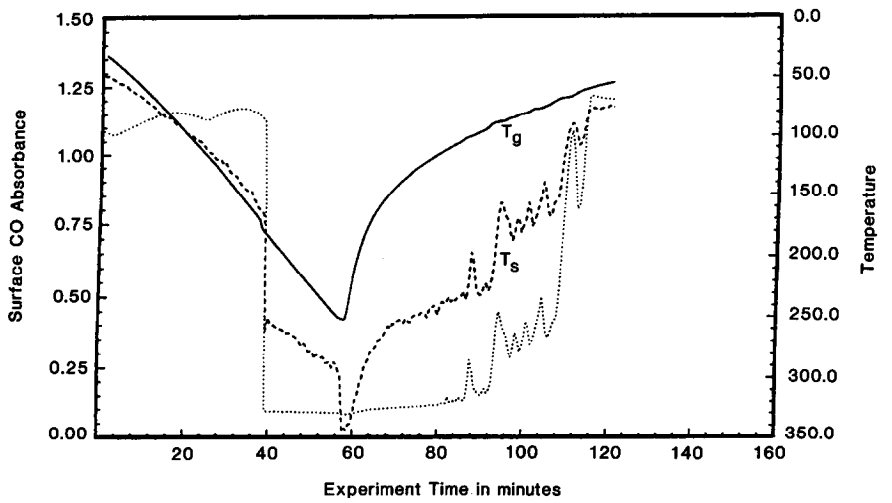

FIG. 5. Temperature-programmed reaction study on a 1% Pt/SiO_2 catalyst. $CO/O_2 = 0.5$, flow rate = 100 ml/min, He = 50%. All temperatures are in °C.

perature oscillations. Figure 8 shows this same effect for a near-stoichiometric CO/O_2 ratio of 1.8. It is important to point out that the phase relationship between CO_2 production, CO surface coverage, and surface temperature is maintained for all of the oscillatory periods studied. The oscillatory periods varied from several seconds to about 7 min. The oscillatory data are summarized in Table 1.

The data in Figs. 6–8 show the strong dependency of the oscillatory periods on gas phase temperature and on the partial pressure of CO. The amplitude of the surface temperature oscillations are maximum for large fluctuations in the surface coverage of CO. The ability of the support temperature to track the rate of CO_2 production strongly suggests that the heat transfer from the supported metal to the support is

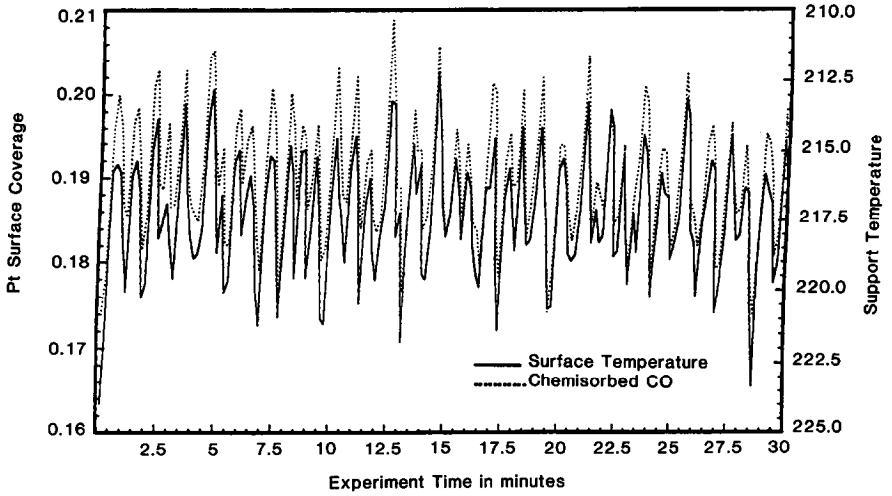

FIG. 6. Support temperature and adsorbed CO coverage oscillations during CO oxidation. $CO/O_2 = 0.5$, $T = 98$°C, flow rate = 100 ml/min, He = 50%. All temperatures are in °C.

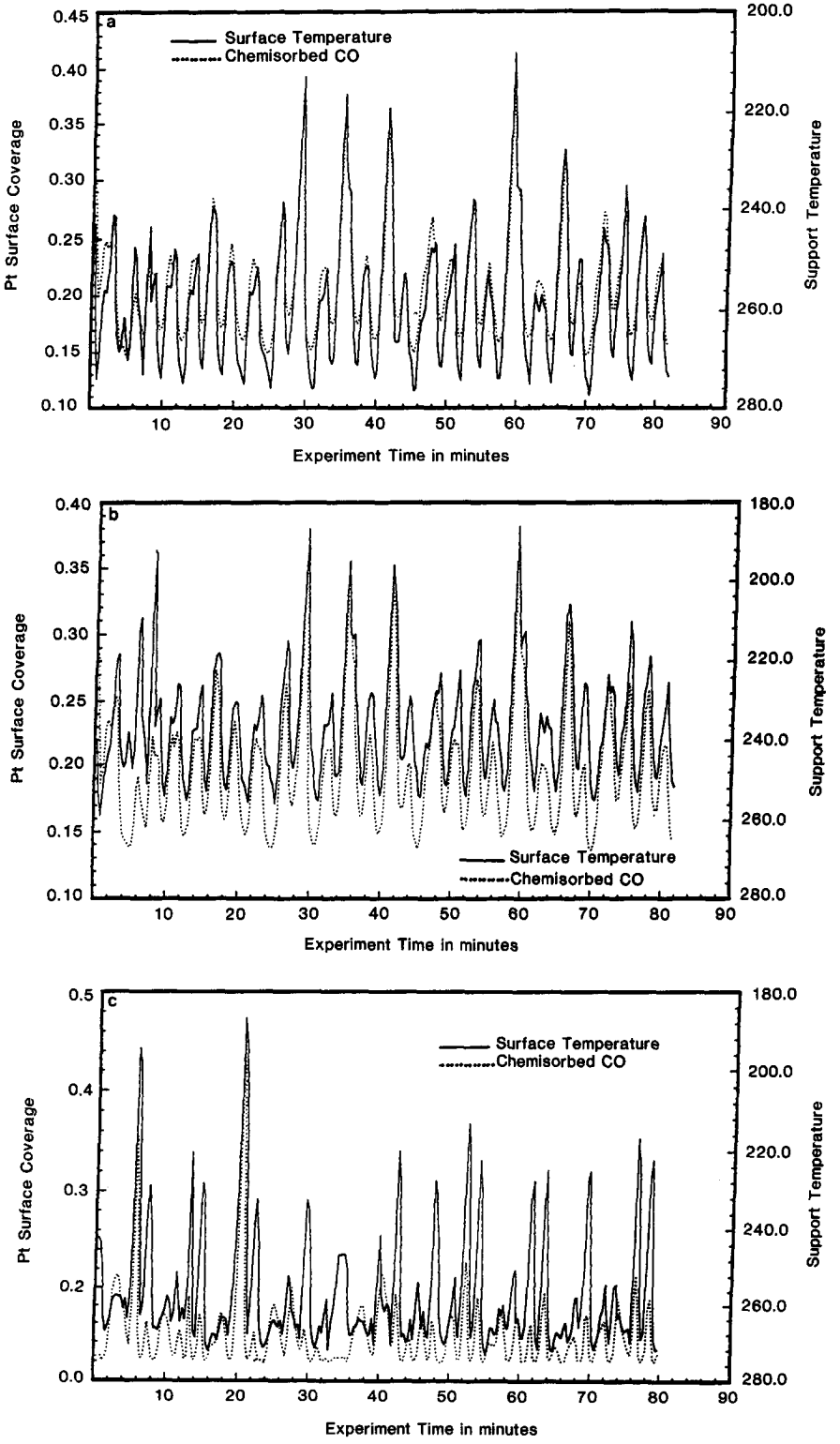

FIG. 7. Support temperatures and adsorbed CO oscillations during CO oxidation. $CO/O_2 = 1.4$, (a) $T = 99°C$, (b) $T = 113°C$, (c) $T = 129°C$, flow rate = 100 ml/min, He = 50%. All temperatures are in °C.

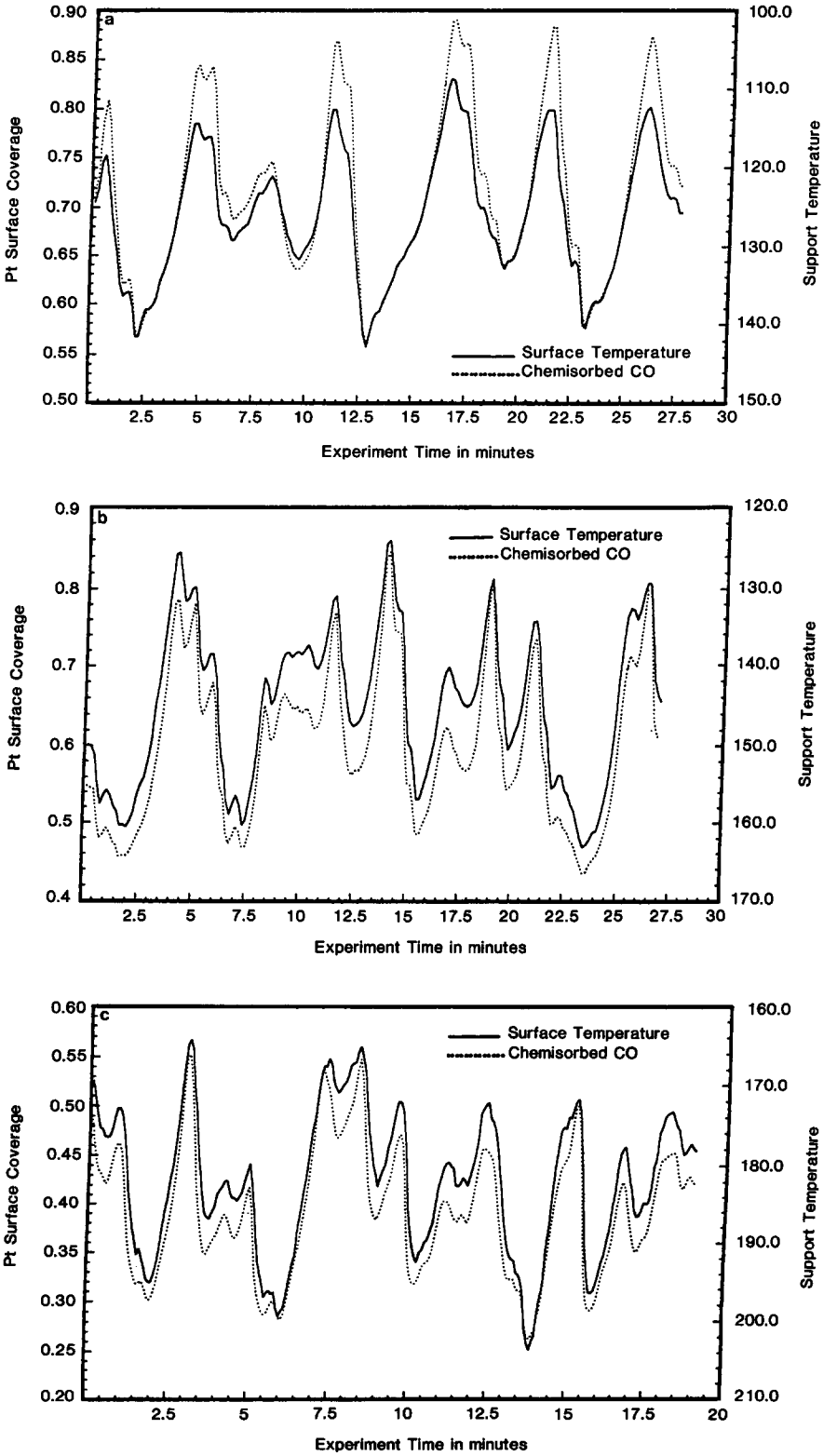

FIG. 8. Support temperature and adsorbed CO oscillations during CO oxidation, $CO/O_2 = 1.8$, (a) $T = 88°C$, (b) $T = 105°C$, (c) $T = 130°C$. All temperatures are in °C.

TABLE 1

Summary of Oscillatory Data

CO/O_2	Gas phase temp (°C)	Oscillation period (min)	T_s (°C)			Surface coverage (%)	
			max	min	ave	max	min
0.5	98	0.5	224	212	217	20	17
1.4	99	4.5	290	200	240	37	15
1.4	119	3.5	265	215	245	30	14
1.4	129	2.0	274	220	255	45	13
1.8	88	4.5	143	106	125	88	56
1.8	105	3.0	164	124	145	85	43
1.8	130	2.5	205	164	185	55	26

very rapid. However, the magnitude of the metal–support temperature gradient still remains unknown.

To determine the magnitude of this temperature gradient a model catalyst consisting of a discontinuous thin Pt film deposited on a quartz crystal was used. This thin Pt film had a resistance of 18Ω at room temperature, increasing to 25Ω when the temperature was raised to 400°C in a flowing 20% O_2/He mixture. The results of this temperature calibration are shown in Fig. 9. The linear relationship was reproducible under conditions of both increasing and decreasing temperature. The calibration was carried out in flowing oxygen to ensure that the resistance measurements obtained during calibration were identical to those present under reaction conditions (i.e., the dependence of film resistance on chemisorbed oxygen is incorporated into the calibration).

The reaction was carried out under steady state conditions with a large excess of O_2. Under these conditions, the CO oxidation reaction is controlled by the rate of

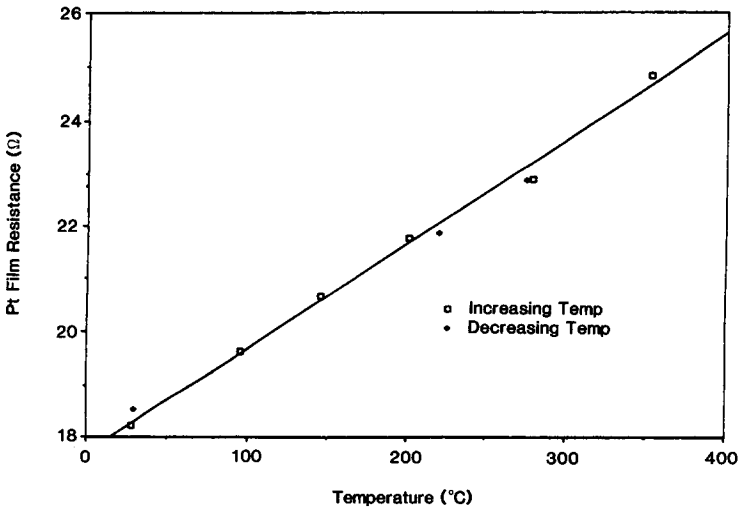

FIG. 9. Pt film resistance calibration.

TABLE 2

Summary of Metal–Support Temperature Gradients

T_{gas} (°C)	T_{metal} (°C)	$T_{support}$ (°C)
121	150	148
200	235	210

diffusion of CO to the surface, so that the surface coverage of CO is negligible (*20*). At higher CO/O_2 partial pressure ratios the adsorption of CO might possibly change the surface resistance measurements. For this reason, oscillations which involve changes in CO surface coverage were avoided.

To determine the magnitude of the metal–support temperature gradient two steady-state CO oxidation reactions were conducted on the thin film catalyst, while resistance and infrared data were collected simultaneously. The first steady-state reaction was carried out at a gas phase temperature of 123°C and the second at a gas phase temperature of 205°C. In both cases the CO/O_2 ratio was fixed at 0.5. For the low conversion reaction, the metal temperature was calculated to be 150°C while the support temperature was 148°C. In the high conversion reaction regime the metal temperature was 235°C and the support was at 215°C. The quartz temperature calibration was carried out in a manner similar to that of the powdered catalyst. The results of this experiment are summarized in Table 2.

DISCUSSION

From the TPR studies (Fig. 5), it is shown that CO oxidation reactions are characterized by three distinct regions of activity. In the first region the reaction has a low conversion rate and consequently the gas–support temperature gradient would be small. In this region the catalyst surface is predominantly covered by CO. As the reaction temperature is increased, the reaction rate increases rapidly and is characterized by a very high conversion of CO. Also, the surface coverage of CO drops to a low value. The temperature at which the reaction enters the second region shifts to higher temperatures with increasing CO/O_2 partial pressure ratios. This is due to the competitive nature of the $CO–O_2$ chemisorption and is described in detail in the literature (*21*). At a CO/O_2 partial pressure of 0.5, this transition occurred at a temperature of 175°C. When this ratio was increased to 1.4, the transition temperature increased to 200°C. Region three is entered upon cooling of the reactor. As the surface cools, the reaction rate decreases and the surface coverage of CO starts to increase. Upon further cooling, the reaction enters the unstable oxidation region which is characterized by sharp fluctuations in the surface coverages of both CO and O_2. The onset of the oscillatory region shifts to lower surface temperatures at lower CO/O_2 partial pressure ratios. At 285°C oscillations were observed for a CO/O_2 ratio of 1.4 while at 260°C oscillatory behavior occurred for a CO/O_2 ratio of 0.5. It is important to note that a shift in the position of the CO IR absorption band never occurred during the course of the CO oscillations. This observation supports the CO island theory proposed by Haaland and Williams (*22*) and Wicke and Boecker (*21*) for the oxidation of CO over Pt/SiO_2.

During the oscillatory oxidation reactions (Figs. 6–8) the intensities of the temperature-dependent bands and the strong surface CO absorbance bands were monitored simultaneously. Using the temperature calibration, the support temperature oscillations were computed. A comparison of the support temperature oscillations to surface CO coverage indicates an inverse relationship between the two; i.e., the periods of the support temperature oscillations are directly out of phase with those of the CO surface coverage. This same intuitive relationship was observed between the reaction rate and the CO surface coverage by Wicke and Boecker (*21*) and between the metal temperature and the effluent CO(g)

phase by Turner *et al.* (*14*). It may be concluded that the metal temperature oscillations and the support temperature oscillations are directly in phase with each other. The oscillation periods observed varied from several seconds to about 7 min and the peak to peak temperature fluctuations were between 10 and 100°C. Also, during many of the experiments, steady-state oscillation data were collected for more than one hour and in all cases surface temperature damping was not observed. In all experiments the temperature and the surface CO concentration were directly out of phase. From these observations a number of conclusions with respect to the metal–support interaction can be made.

This phase relationship, along with the ability of the surface to track large temperature changes, indicates that the metal–support interaction is important and cannot be neglected as has been done in numerous analytical studies in the past. The ability of the support to follow the large temperature fluctuations is an indication that the support is predominantly responsible for heat dissipation from the metal, rather than convective cooling of the metal by the gas, as had previously been assumed. Also, due to this rapid heat transfer, the metal–support temperature gradient should also be small as concluded by Holstein and Boudart (*5*). However, the mechanism by which heat is transferred would most certainly be different from the one proposed by them.

In the measurement of metal-temperature gradients two steady-state reaction regimes were considered. As noted in the TPR study, CO coverage reactions below 185°C are characterized by low conversion and, therefore, less metal surface heating. Above this temperature the oxidation reaction enters a region where the conversion becomes very large. By considering both these regions an upper limit to the metal–support gradient that can exist in powdered catalyst may be established. In the low conversion region, it was observed that the metal–support gradient was only a few degrees. This was less than the resolution of the infrared technique. In the high conversion region, the metal–support gradient was found to be a maximum of 20°C.

The temperature gradient measured during these thin film experiments represents the maximum temperature gradient which may be present in a powdered catalyst. In a powdered catalyst pellet, the active metal sites are imbedded and distributed in a silica particle which in turn is incorporated into a pellet. This arrangement allows greater contact possibilities to exist between the metal and the support than in the case of the thin film model catalyst. For this reason, the heat transfer in the powdered pellet should be much more efficient than in the thin film sample and consequently the temperature gradient should be considerably smaller.

CONCLUSIONS

The following important conclusions emerge from this study:

(1) Metal–support temperature gradients in a supported catalyst are small.

(2) Heat transfer from the metal to the support is very rapid.

(3) The primary mode of heat dissipation by the metal particles is by conduction to the support, much as Holstein and Boudart (*5*) have suggested.

(4) Convection from the support to the gas is the primary method by which the catalyst bed is cooled.

(5) Thermal contact between the metal crystallites and the carrier particle is much more efficient than has previously been assumed.

ACKNOWLEDGMENTS

We acknowledge support from the Petroleum Research Fund of the American Chemical Society under Grant 14377-AC-5 for this research. We also thank Mr. Lambert Lucietto of the Byron-Lambert Co., Franklin Park, Illinois, for his much needed input in overcoming numerous technical problems associated with the reactor design. Finally, we are grateful to the U.S. Department of Energy (Grant DOE-FG02-86ER-13531), who supplied funds for the purchase of a large portion of the equipment used in this research.

REFERENCES

1. Luss, D., *Chem. Eng.* **1,** 311 (1970).
2. Chan, S. H., Low, J. D., and Mueller, W. C., *AIChE J.* **17,** 1499 (1971).
3. Ruckenstein, E., and Petty, C. A., *Chem. Eng. Sci.* **27,** 938 (1972).
4. Steinbruchel, C. H., and Schmidt, L. D., *Surf. Sci.* **40,** 693 (1973).
5. Holstein, W. L., and Boudart, M., *Rev. Latinoam. Ing. Quim. Quim. Apl.* **13,** 107 (1983).
6. Kember, D. R., and Sheppard, N., *J. Chem. Soc. Faraday Trans.* **77**(2), 1321 (1981).
7. Cale, T. S., and Ludlow, D. K., *Anal. Instrum.* **13,** 183 (1984).
8. Cale, T. S., Richardson, J. T., and Ginestra, *J. Appl. Phys. Lett.* **42,** 744 (1983).
9. Cale, T. S., and Richardson, J. T., *J. Catal.* **79,** 378 (1984).
10. Cale, T. S., *J. Catal.* **90,** 40 (1984).
11. Matyi, R. J., Butt, J. B., and Schwartz, L. H., *J. Catal.* **91,** 185 (1985).
12. Kaul, D. J., and Wolf, E. E., *J. Catal.* **91,** 216 (1985).
13. Kaul, D. J., and Wolf, E. E., *J. Catal.* **93,** 321 (1985).
14. Turner, J. E., Sales, B. C., and Maple, M. B., *Surf. Sci.* **103,** 54 (1981).
15. Kember, D. R., and Sheppard, N., *J. Chem. Soc. Faraday Trans.* **77,** 1309 (1981).
16. Miura, H., and Gonzalez, R. D., *J. Phys. Ed. Sci. Instrum.* **15,** 373 (1983).
17. Boecker, D., Ph.D. dissertation, University of Muenster, West Germany, 1985.
18. Sarkany, J. A., and Gonzalez, R. D., *J. Catal.* **75,** 75 (1982).
19. Benziger, J. C, McGovern, S. J., and Royce, B. S. H., *Catal. Charact. Sci.* **38,** 449 (1985).
20. Saymeh, R., and Gonzalez, R. D., *J. Phys. Chem.* **90,** 4819 (1986).
21. Wicke, E., and Boecker, D., *Ber. Bunsen.-Ges. Phys. Chem.* **89,** 629 (1985).
22. Haaland, D. M., and Williams, F. L., *J. Catal.* **76,** 450 (1980).